Available online at www.sciencedirect.com
ScienceDirect
J. Genet. Genomics 36 (2009) 133−140
JOURNAL OF GENETICS AND GENOMICS
www.jgenetgenomics.org

Differentiation potential of bone marrow mesenchymal stem cells in duck

Linfeng Li [a, b], Xiujuan Bai [b], Xuelian Gong [a], Hongkun Liu [a], Lina Chen [a], Weijun Guan [a, *], Yuehui Ma [a, *]

[a] *Institute of Animal Science, Chinese Academy of Agricultural Science, Beijing 100193, China*
[b] *College of Animal Science and Technology, Northeast Agricultural University, Harbin 150000, China*

Received for publication 20 September 2008; revised 21 January 2009; accepted 23 January 2009

Abstract

The bone marrow mesenchymal stem cells (MSCs) are multipotent stem cells which can differentiate into mesenchymal cells *in vitro*. In this study, MSCs in duck were isolated from bone marrow by density gradient centrifuge separation, purified and expanded in the medium. The primary MSCs were expanded for 11 passages. The different-passage MSCs were induced to differentiate into osteoblasts and neuron-like cells. Karyotype analysis indicated that MSCs kept diploid condition and the hereditary feature was stable. The different-passage MSCs expressed CD44, ICAM-1 and SSEA-4, but not CD34, CD45 and SSEA-1 when detected by immunofluorescence staining. There was no significant difference among the positive rates of passages 2, 6 and 8 ($P > 0.05$), but a significant difference existed among those of passages 2, 6, 8 and 11 ($P < 0.05$). After the osteogenic inducement was added, the induced different-passage MSCs expressed high-level alkaline phosphatase (ALP), and are positive for tetracycline staining, Alizarin Red staining and Von Kossa staining. After the neural inducement was added, about 70% cells exhibited typical neuron-like phenotype, the induced different-passage MSCs expressed Nestin, neuron-specific enolase (NSE) and glial fibrillary acidic protein (GFAP) when detected by immunofluorescence staining. There was no significant difference among the positive rates of passages 3, 4 and 6 ($P>0.05$), but a significant difference existed among those of passages 3, 4, 6 and 8 ($P<0.05$). These results suggest that MSCs in duck were capable of differentiating into osteoblasts and neuron-like cells *in vitro*.

Keywords: duck; mesenchymal stem cells; induction; differentiation

Introduction

Bone marrow mesenchymal stem cells (MSCs) are generally known as ancestors of bone marrow stromal cells, which can assist hematopoiesis. Recently, MSCs were found to be more effective in their differentiation potential in that they were able to give rise to many kinds of mesenchymal cells, such as osteoblast, chondrocyte, tenocyte, adipocyte and cardiac myocyte, etc (Prockop et al., 1997; Pittenger et al., 1999). Furthermore, they were even able to differentiate into neurocyte which derived from the ectoderm (Woodbury et al., 2000). MSCs expressed numerous surface markers such as SH2, SH3, CD29, CD90, CD106 and CD166, but not hematopietic markers such as CD14, CD34 and CD45 (Deans and Moseley, 2000). MSCs could be expanded in culture and cryopreserved without loss of phenotype or multilineage differentiation potential (Majumdar et al., 1998). It was indicated in recent studies that MSCs were capable of homing to the bone marrow of non-human primates following systemic infusion (Devine

* Corresponding author. Tel: +86-10-6281 5992; Fax: +86-10-6281 3463.
E-mail address: wjguan86@126.com (W. Guan);
yuehui.ma@263.net (Y. Ma)

DOI: 10.1016/S1673-8527(08)60100-9

et al., 2001). All the results mentioned above suggest that MSCs might be useful in cell therapy, gene therapy and tissue engineering.

MSCs are useful model system for better understanding of cell behavior and differential gene expression in the context of a focused and easily manipulated biological system. The continued understanding of cellular origin and MSCs' behavior will enable further identification of diagnostic markers and therapeutic targets. MSCs assist gene transfer, so that they can be used to produce medical antibodies. In addition, it is easy to obtain MSCs of duck, and MSCs are suitable for large scale preparation and are an ideal medicine screening model for the treatment of cell diseases. Therefore, MSCs of duck were chosen as our experimental material.

In this study, we examined the biological characteristics of MSCs and further evaluated the feasibility of inducing the differentiation of MSCs into osteoblasts and neuron-like cells *in vitro*. To characterize the differentiated MSCs, we examined their morphology and analyzed several markers at different passages after induction by means of histochemistry and immunofluorescence methods, which provides a theoretical foundation and a technological method for the utilization of MSCs.

Materials and methods

Isolation, purification and expansion of MSCs

Bone marrow samples were drained from the tibia of one-day-old ducks. Firstly, cells were pelleted by centrifugation, then resuspended with PBS and fractionated on a density gradient (Ficoll-Hypaque, 1.077 g/mL, Amersharm Biosciences, Sweden) for 20 min at 400 g. The interface was collected and seeded at 1.0×10^6 cells/cm^2 in T-25 flasks with 5 mL L-DMEM (Stem Cell Co., Canada). Cultures were maintained at 37.5°C in a humidified atmosphere containing 95% air and 5% CO_2. The non-adherent cells were removed after three days and the culture medium was changed every 3 days. When cultures became 80% confluence, cells were detached with 0.25% trypsin and 0.02% EDTA (1:1) for 3–5 min at 37.5°C, and reseeded at 8.0×10^3 cells/cm^2 in T-25 flasks with 5 mL L-DMEM for serial passaging.

Growth dynamical analysis of MSCs

MSCs of passages 2, 6 and 8 were harvested and made into cell suspensions, incubated in 24-well plates at the same concentration, and then put into an incubator containing CO_2 of 0.05 volume fraction at 37.5°C. The culture medium was changed every 3 days. MSCs in 3 culture foramens were randomized every day for the cell growth dynamical analysis and the growth curve of different-passage MSCs was drawn.

Chromosome analysis

Cells were harvested at 80%–90% confluence during their exponential growth phase, and microslides were prepared and the chromosome staining was performed according to the approach described (Hirofumi et al., 2006). The number of chromosomes in 50 to 100 spreads was counted. The three important chromosomal parameters, i.e., relative length, arm ratio and centromere index, were calculated by the method proposed by Kawarai et al. (2006).

Surface antigen characteristics of MSCs

Surface antigens of the different passages of MSCs were detected by immunofluorescence staining. MSCs of passages 2, 6, 8 and 11 were fixed in 4% paraformaldehyde/PBS for 15–20 min, and then blocked for 10 min with methanol containing 0.1% Triton X-100 and 0.3% peroxid (H_2O_2) to eliminate endogenetic peroxides, incubated in goat serum working solution for 15 min to block nonspecific binding, then the MSCs were incubated with primary antibodies at 4°C overnight. The MSCs were incubated with secondary antibodies which were conjugated with FITC (goat anti-mouse IgG). For negative control, 0.01 mol/L PBS was used to replace primary antibodies. For blank control, MSCs were stained directly. Fluorescence images were observed by fluorescence microscope. Ten non-overlapped visions (×100) were randomized from different-passage MSCs, then the percentage of positive cells relative to total count of MSCs was calculated and the results were expressed as mean ± SD using SPSS 10.0 software for variance analysis.

Differentiation of MSCs into osteoblasts

MSCs of passages 3, 4, 6 and 8 were vaccinated in a 24-well plate at 3×10^3 cells/cm^2. These MSCs were divided into two groups when covering 80% surface of the culture plate. MSCs in the induction group were incubated in the medium of inducers (10 mmol/L β-sodium glyc-

erophosphate, 10^{-8} mmol/L dexamethasone, 50 mg/L vitamin C) containing osteoblasts. MSCs in the control group were incubated in the medium of inducers without osteoblasts. Culture medium was changed every 3 days. Two weeks later, alkaline phosphatase levels were measured by the Gomori Ca-Co method. Three weeks later, Alizarin Red staining was used to determine calcium nodus. Four weeks later, Von Kossa and tetracycline fluorescence labeling of calcium were used to determine calcium nodus.

Differentiation of MSCs into neural cells

The preparation of MSCs was the same as that mentioned above. MSCs in the induction group were induced with 20% fetal bovine serum, 3 μmol/L β-mercaptoethanol (BME, Sigma, USA) for 24 h, washed thrice with PBS, and then induced with serum-free medium containing 2% dimethyl sulphoxide (DMSO, Sigma) and 200 μmol/L butylated hydroxyanisole (BHA, Sigma). MSCs in the control group were incubated with serum medium.

The immunofluorescence staining was the same as that mentioned above. The primary antibodies were Nestin, NSE and GFAP. The secondary antibodies were conjugated with FITC and Cy5, respectively. For the control group, 0.01 mol/L PBS was used to replace primary Nestin, NSE, and GFAP antibodies. Ten non-overlapped visions (×100) were randomized from induced stained cells, followed by the same data processing as that mentioned above.

Results

Isolation, culture and proliferation of MSCs

MSCs were round, large, lucent and with strong refraction. Nuclei were oval and mixed with some blood cells. The non-adherent cells were removed on the third day and MSCs were fusiform and showed cell-like clone with growth being slower (Fig. 1A). Four days later, MSCs proliferated rapidly. On the 7th day of primary culture, the cells exhibited either an osteoclast-like or a mesenchymal-like phenotype. Cells with the osteoclast phenotype were large, oval/round-shaped and multinucleated. Cells with the mesenchymal phenotype were homogeneous, and displayed fibroblast-like and bipolar spindle-shape (Fig. 1B). Twelve to fourteen days later, cell appearance was

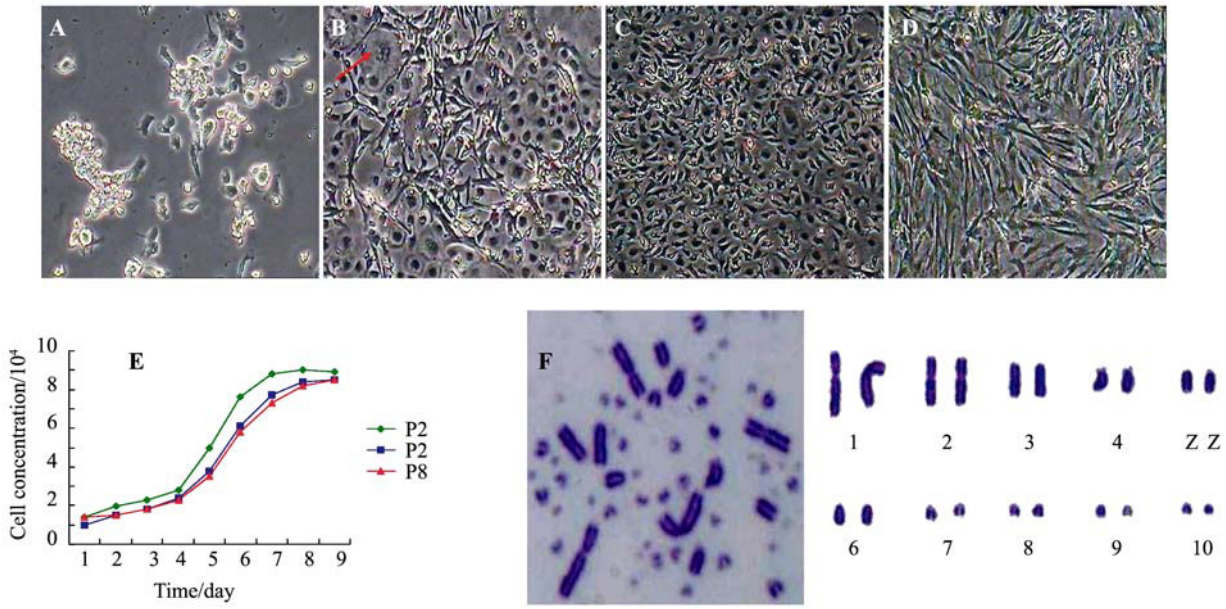

Fig. 1. Morphology, growth curve and karyotype of MSCs. **A:** on the 3rd day of primary culture, MSCs were round with clear boundaries and with growth being slower (100×). **B:** on the 7th day of primary culture, MSCs were in the star, polygon or long shuttle shape, most of which have protrusions and cells gradually converged (100×, red arrowhead is osteoclast) **C:** MSCs of the passage 3; cells were arranged like fibroblast, and almost the same and appeared to be in the shuttle shape (100×). **D:** MSCs of the passage 9; cells were homogeneous and typical long spindle-shape. **E:** the growth curves of passages 2, 6 and 8 of MSCs were observed for comparison. The growth curve of the different-passage MSCs appeared as a typical "S" shape with cell density on the left axis. Growth curve included latency phase, exponential growth phase and stationary phase. **F:** chromosome at metaphase (left) and karyotype (right) of MSCs (♂) (1,000×). 2n chromosomes number of MSCs was 78, consisting of 10 pairs of macrochromosomes and 28 pairs of microchromosomes, whilst the sex chromosome type was ZZ (♂).

more similar when 80% confluence was achieved. MSCs grew rapidly and presented representative fibroblast after passaging. Then seven to ten days later, MSCs could adhere to the whole bottom of the culture flask, arrange in swirl till confluence. MSCs were passaged for eleven times. The different-passage MSCs did not change obviously in morphology and were stable in property after passaging (Fig. 1, C and D). Therefore, it was feasible for the proliferation of MSCs *in vitro*. After 10-passage cultures, aging signs appeared in MSCs, such as retarded growth of cell, pyknosis and karyopyknosis of most cells and dropped-out from culture plate.

The growth curves of passages 2, 6 and 8 of MSCs were S-shaped (Fig. 1E). Two or three days later, MSCs entered the exponential growth phase, and seven to nine days later, entered platform growth phase. In views of growth curves of different-passage MSCs, MSCs are suitable for the experiment in early period of passage.

Chromosome analysis of MSCs

As the chromosomes are small and difficult to differentiate, we sampled 100 cells. The number of chromosomes in the duck MSCs was 2n=78, consisting of 10 pairs of macrochromosomes and 28 pairs of microchromosomes, whilst the sex chromosome type was ZZ (♂)/ZW (♀). Chromosomes 1 and 4 were classified as type SM; chromosome 2 was classified as type M; chromosomes 3, 6, 7, 8, 9 and 10 were classified as T and the sex chromosome was Z/W (male ZZ and female ZW). Z and W chromosomes were classified as type T. The Z chromosome was as large as chromosome 4 whilst the W chromosome was of similar size to chromosome 8. These results were consistent with the varietal characteristics of duck (Fig. 1F).

Surface antigen characteristics of MSCs

Immunofluorescence staining results showed that different passages of MSCs expressed antigens CD44 (Fig. 2, A and A_1), ICAM-1 (Fig. 2, B and B_1) and SSEA-4 (Fig. 2, C and C_1), but did not express antigens CD34 (Fig. 2, D and D_1), CD45 (Fig. 2, E and E_1) and SSEA-1 (Fig. 2, F and F_1). There was no significant difference in the positive rates of passage 2, 6 and 8 (P>0.05), but significant difference was present among passages 2, 6, 8 and 11 (P<0.05, Table 1). CD34 and CD45 antigens are hematopietic markers. CD44 is a type I transmembrane glycoprotein expressed in many types of cells, including B cells, most T cells, monocytes and some epithelial cells. It is implicated in various processes, such as hematopoiesis, lymphocyte homing, leukocyte activation. The results suggested that the MSCs are a group of uncommited stem/progenitor cells which differ from mesenchymal cells.

MSCs after the induction with osteoblast inducers

After the induction with osteoblast inducers, MSCs had significant changes in appearance. From the 3rd day after the induction, some MSCs changed from fusiform to three-dimensional, becoming larger and changing into polygon. As time went by, triangle or polygonal cells

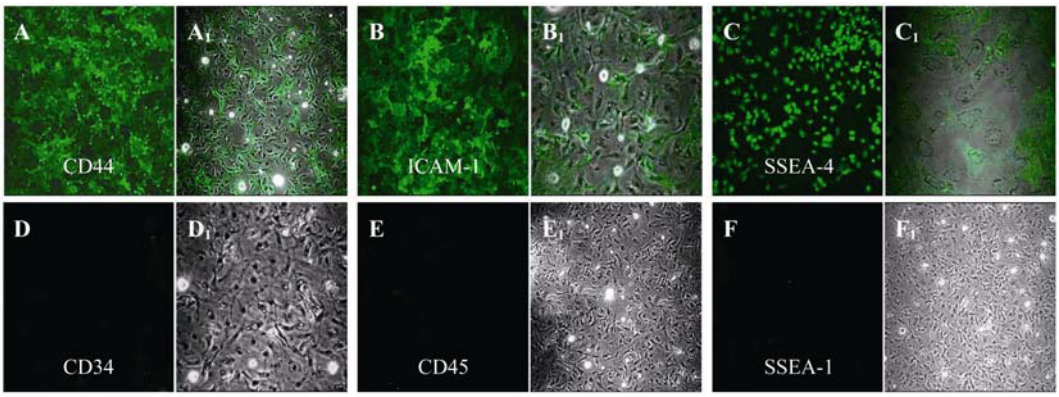

Fig. 2. Surface antigen characteristics of the passage 2 MSCs (100×). MSCs express numerous surface markers such as CD44, ICAM-1 and SSEA-4, but no hematopietic markers such as CD34, CD45 and SSEA-1. **A:** MSCs were positive in CD44 expression. **B:** MSCs were positive in ICAM-1 expression. **C:** MSCs were positive in SSEA-4 expression. **A_1–C_1:** merged with phase and immunofluorescence for CD44, ICAM-1 and SSEA-4 of the passage 2 MSCs **D:** MSCs were negative in CD34 expression. **E:** MSCs were negative in CD45 expression. **F:** MSCs were negative in SSEA-1 expression. **D_1–F_1:** phase images of the passage 2 MSCs.

Table 1
Positive rates of CD44, ICAM-1 and SSEA-4 expressions of passages 2, 6, 8 and passage 11 by immunofluorescence staining

Surface antigen	Passage 2	Passage 6	Passage 8	Passage 11
CD44	86.3 ± 2.4	85.2 ± 1.8	84.6 ± 1.3	38.0 ± 2.8
ICAM-1	83.1 ± 1.4	82.8 ± 2.0	81.4 ± 2.6	28.9 ± 1.7
SSEA-4	43.8 ± 2.4	42.6 ± 1.1	41.9 ± 2.5	10.4 ± 1.8

SPSS 10.0 software analysis was used to compare positive rates of surface antigen at four different-passage MSCs, and the differences in the positive ratio between passages 2, 6, 8 and passage 11 were significant ($P<0.05$). The comparisons of means among multiple samples were performed. The mean of passage 11 had significant difference with those of passages 2, 6 and passage 8 ($P<0.05$); the mean of passage 2 had no significant difference with those of passage 6 and passage 8 ($P>0.05$).

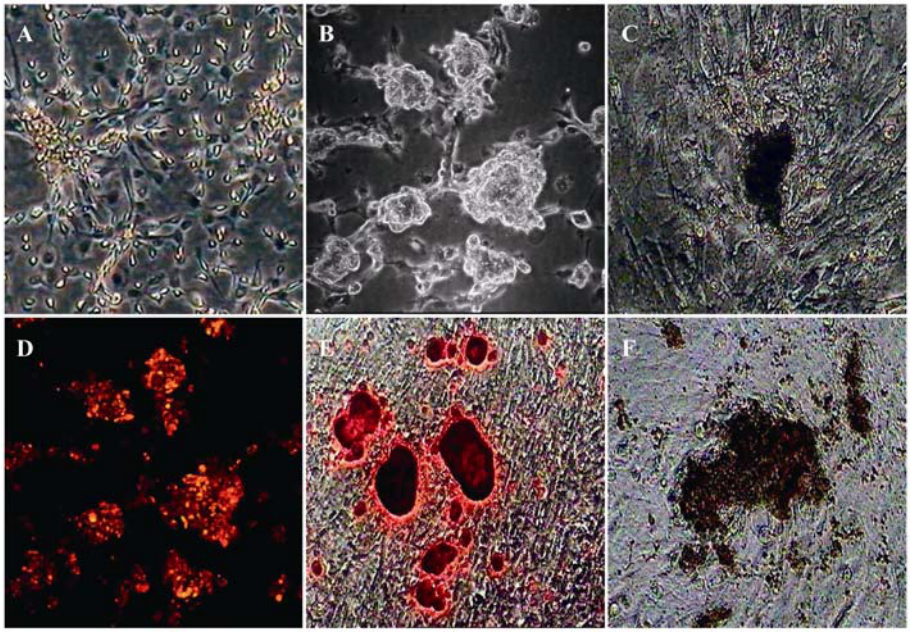

Fig. 3. Identification of osteogenic differentiation of the passage 3 MSCs. **A:** the 9-day culture of induction group (100×). **B:** osteogenesis induction for 21 days (100×). **C:** AKP determined by the Gomori Ca-Co method two weeks after MSCs induction (100×). **D:** tetracycline label of induction group (100×). **E:** opacity deposition in the center of cell clones could be stained scarlet red mottling by Alizarin Red three weeks after MSCs induction (100×). **F:** Von Kossa staining positive four weeks after MSCs induction, a characteristic for calcium salt staining (100×).

increased, and then grew into multilayers, and many crystal particles could be seen (Fig. 3, A and B). Alkaline phosphatase level was determined by the Gomori Ca-Co method two weeks after MSCs induction. Brown-black particles were found to be present in cytoplasm (Fig. 3C). Under the fluorescence microscope, the calcium nodules were golden mass (Fig. 3D), and fluorescence intensity gradually enhanced. It indicated that the calcium salt crystal deposition in the extracellular matrix gradually increased. On the forth week the induced cells were stained with Alizarin Red, which was positive with the positive region being bright red (Fig. 3E). With the culture days increasing, the number of nodules gradually increased, and Von Kossa staining was positive (Fig. 3F).

Induced differentiation of MSCs into neuron-like cells

MSCs were preinduced for 24 h. After 24 h, the spindle-shaped cells begun to contract and changed to irregular shapes (Fig. 4A). Once the induction began, cell bodies further contracted and became round, triangular or cone-shaped during multipolar processes. Processes continued to elaborate, displaying many branches, growth cone-like terminal expansions. Some cells underwent a long process with evident varicosities, similar to the long axon of Golgi I neuron (Fig. 4B). The cell morphology became stable after 6 h. Microscopic observation showed about 70% cells exhibited a typical neuron-like morphology (Fig. 4C).

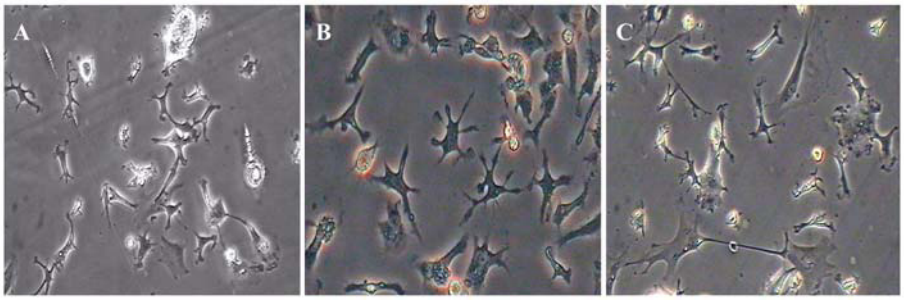

Fig. 4. Morphologic changes in differentiating neuron-like cells. **A:** preinduction for 24 h (40×), MSCs became irregular-shaped. **B:** induction for 3 h (100×), MSCs became round, triangular or cone-shaped. **C:** induction for 6 h (40×), MSCs became similar to the long axon of Golgi I neuron, displayed a typical neuron-like morphology.

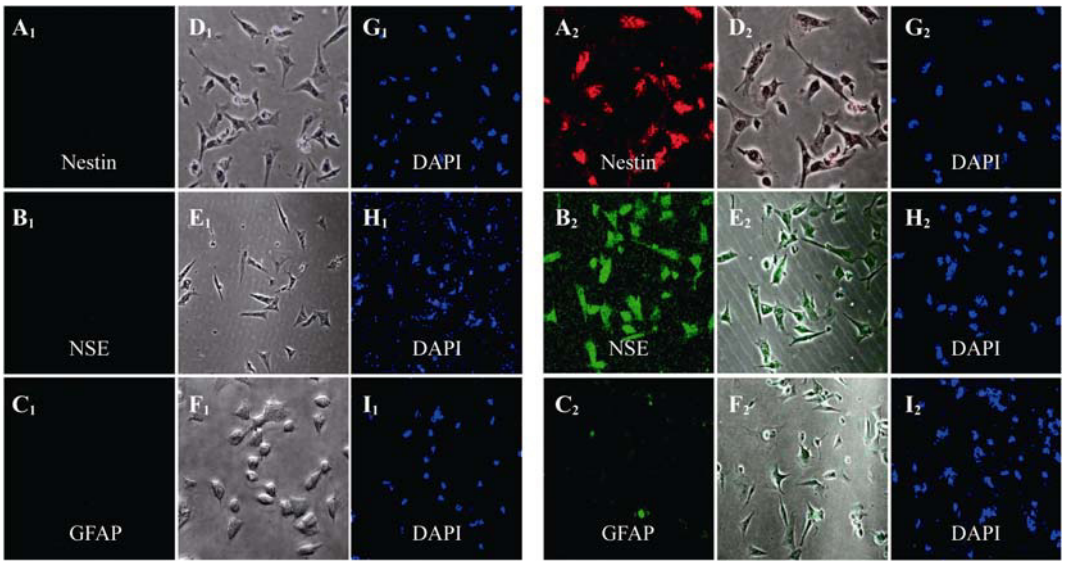

Fig. 5. Immunofluorescence images of Nestin, NSE and GFAP after the passage 3 of MSCs intervened with neural cell inducer in 6 h. **A_1:** Nestin negative control (100×). **B_1:** NSE negative control (100×). **C_1:** GFAP negative control (200×). **D_1–F_1:** phase images of negative control (100×). **G_1–I_1:** DAPI nuclear counterstained untreated MSCs (100×). Blue indicates DAPI. **A_2:** induced MSCs were positive in Nestin expression (40.1% ± 2.2%) (200×). **B_2:** induced MSCs were positive in NSE expression (82.7% ± 8%) (100×). **C_2:** induced MSCs were positive in GFAP expression (4.8% ± 1.4%) (100×). There were remarkably difference in positive rates of different surface antigens expression (P<0.05). **D_2–F_2:** merged with phase and immunofluorescence for Nestin ,NSE and GFAP of induced MSCs (200×). **G_2–I_2:** DAPI nuclear counterstained induced MSCs (200×). Blue indicates DAPI.

It was indicated by the immunofluorescence staining detection that non-induced MSCs did not express Nestin (Fig. 5, A_1, D_1 and G_1), NSE (Fig. 5, B_1, E_1 and H_1) and GFAP (Fig. 5, C_1, F_1 and I_1). After 6 h of induction, all MSCs in different passages expressed Nestin (Fig. 5, A_2, D_2 and G_2), NSE (Fig. 5, B_2 , E_2 and H_2) and GFAP (Fig. 5, C_2, F_2 and I_2). The positive rates (the count of cells positive for Nestin, NSE and GFAP under microscope, randomized for 5 times) of Nestin, NSE and GFAP expression during the induction and differentiation of different-passage MSCs were presented in Table 2. The results indicated that passages 3, 4, and 6 of MSCs all expressed Nestin, NSE and GFAP, and there was no significant difference among the positive rates of different-passage MSCs (P>0.05). In the induced passage 8 of MSCs, the positive rates of Nestin, NSE and GFAP decreased remarkably, indicating a significant difference existed among those of passages 3, 4, 6 and 8 (P<0.05). The difference resulted from the aging signs presented when MSCs were proliferated to passage 8, which affected the cell transformation.

Table 2
Positive rates of Nestin, NSE and GFAP expressions after differentiation of MSCs of passages 3, 4, 6 and 8 to neurons in 6 h

Surface antigen	Passage 3	Passage 4	Passage 6	Passage 8
Nestin	40.1 ± 2.2	39.2 ± 2.0	39.6 ± 2.3	10.0 ± 1.8
NSE	82.7 ± 1.8	81.4 ± 2.1	80.4 ± 2.3	18.8 ± 1.9
GFAP	4.8 ± 1.4	4.8 ± 1.8	4.7 ± 2.1	0.4 ± 1.1

SPSS 10.0 software analysis was used to compare positive rates of surface antigen at four different-passage MSCs, and the difference in the positive ratio between passages 3, 4, 6 and 8 was significant ($P<0.05$). The comparisons of means among multiple samples were performed. The mean of the passage 8 had significant difference with those of passages 3, 4 and passage 6 ($P<0.05$); the mean of the passage 3 had no significant difference with those of passage 4 and passage 6 ($P>0.05$).

Discussion

Cell therapy has emerged as a strategy for the treatment of many human diseases. At present, tissue stem cells were tentatively expanded and orientationally induced *in vitro* to some cells that are needed, which are then implanted into patients to repair damage, to replace regressive tissue and improve the function of hereditarily defective tissue. The transplantation of hematopoietic stem cell has been widely used in the treatment of hematopoietic malignent diseases, which provides an exemplification for the study of tissue stem cells. It was reported that MSCs could be used to repair and reconstruct some tissues such as bone cartilage, lung, brain, etc (Pereira et al., 1998). Human MSCs cultured *in vitro* were implanted into rat brains (Azizi et al., 1998). Results showed that MSCs cultures could migrate along neural stem cell pathways and survive in a manner similar to rat astrocytes. Adult rat and human MSCs cultures induced *in vitro* differentiate into neurons (Deans et al., 2000). In addition, MSCs assist gene transfer and megakaryocyte and pro-platelet formation from CD34+ hematopoietic progenitor cells (Reese et al., 1999; Cheng et al., 2000).

At present, the number of MSCs in mononuclear cells is not enough for tissue engineering. Accordingly, it is necessary to expand and purify MSCs *in vitro*. *In vivo*, the development and obtaining function of tissue stem cells are related to gene-encoded transcription factors and extracellular signals (Majumdar et al., 1998). However, *in vitro,* the differentiation mechanism of tissue stem cells is not clear yet. In this study, we performed the differentiation of MSCs into neurocytes *in vitro*. Firstly, we preinduced MSCs with L-DMEM medium containing 20% FBS and 3 μmol/L β-mercaptoethanol, and then formally induced them to differentiate into neurocytes with an induction medium composed of L-DMEM/2% DMSO/200 μmol/L BHA. Both β-mercaptoethanol and BHA were antioxidants, and BHA was stronger than β-mercaptoethanol (Woodbury et al., 2000). BHA and β-mercaptoethanol could assist the viability and differentiation of MSCs. But the functional roles of BHA are not known at present. It was indicated that the optimal concentration (10 to 50 μmol/L) of β-mercaptoethanol added in a serum-free medium exhibited a prominent effect on the survival of neurons. The survival rate of neurons increased approximately from several to hundreds of folds, which was related to the antioxidation of β-mercaptoethanol (Ishii et al., 1993). The above results indicated that MSCs had strong expansion capacity *in vitro* and differentiation potential to mesenchymal and non-mesenchymal cells and might be a new approach for cellular and gene transfer treatment.

In different induction conditions, MSCs differentiated to different lineage cells. It was indicated that the ambience affected and decided the lineage specificity and committed differentiation of cells. The specific tissue stem/ancestor cells can differentiate into various cells of identical germ layer and different germ layer. MSCs are typical examples. They come from mesoblast, but they can differentiate into mesoblast and nerve ectoderm tissue cells *in vitro*, such as osteocytes, adipocytes, neurocytes, etc. However, at present, committed differentiation mechanism *in vitro* of MSCs is not entirely clear. Further study of differentiation mechanism will promote the utilization of MSCs in cell and gene therapy.

In summary, it is indicated that MSCs of duck have the capability of differentiating into osteoblasts and neuron-like cells when induced *in vitro*. This potential may represent a novel candidate resource for cellular transplant therapy of nervous system disease and bone tissue engineering. However, this study only investigated the morphology and phenotype of differentiated osteoblasts and neuron-like cells, and the cells still need to be further identified according to their functional characteristics, which will be accomplished in our future work.

Acknowledgments

This work was supported by the National High-Tech Research and Development Program of China (863 Program) (No. 2006AA10Z198 and 2007AA10Z170), the National Infrastructure of Natural Science and Technology Program (No. 2005DKA21101) and the National Scientific Foundation of China (No. 30671539).

References

Azizi, S.A., Stokes, D., Augelli, B., DiGirolamo, C., and Prockop, D.J. (1998). Engraftment and migration of human bone marrow stromal cells implanted in the brains of albino rat—similarities to astrocyte grafts. Proc. Natl. Acad. Sci. USA **95:** 3908–3913.

Cheng, L., Qasba, P., Vanguri, P., and Thiede, M.A. (2000). Human mesenchymal stem cells support megakaryocyte and pro-platelet formation from CD34(+) hematopoietic progenitor cells. J. Cell Physiol. **184:** 58–69.

Deans, R.J., and Moseley, A.B. (2000). Mesenchymal stem cells: Biology and potential clinical uses. Exp. Hematol. **28:** 875–884.

Devine, S.M., Bartholomew, A.M., Mahmud, N., Nelson, M., Patil, S., Hardy, W., Sturgeon, C., Hewett, T., Chung, T., Stock, W., Sher, D., Weissman, S., Ferrer, K., Mosca, J., Deans, R., Moseley, A., and Hoffman, R. (2001). Mesenchymal stem cells are capable of homing to the bone marrow of non-human primates following systemic infusion. Exp. Hematol. **29:** 244–255.

Hirofumi, S., Kentaro, Y., Kouichi, H., Tsuyoshi, F., Norihiro, T., and Norio, N. (2006). Efficient establishment of human embryonic stem cell lines and long-term maintenance with stable karyotype by enzymatic bulk passage. Biochem. Biophys. Res. Commun. **345:** 926–932.

Ishii, K., Katayama, M., Hori, K., Yodoi, J., and Nakanishi, T. (1993). Effects of 2-mercaptoethanol on survival and differentiation of fetal mouse brain neurons cultured *in vitro*. Neurosci. Lett. **163:** 159–162.

Kawarai, S., Hashizaki, K., Kitao, S., Nagano, S., Madarame, H., Neo, S., Ishikawa, T., Furuichi, M., Hisasue, M., Tsuchiya, R., Tsujimoto, H., and Yamada, T. (2006). Establishment and characterization of primary canine hepatocellular carcinoma cell lines producing alpha-fetoprotein. Vet. Immunol. Immunopathol. **113:** 30–36.

Majumdar, M.K., Thiede, M.A., Mosca, J.D., Moorman, M., and Gerson, S.L. (1998). Phenotypic and functional comparison of cultures of marrow-derived mesenchymal stem cells (MSCs) and stromal cells. J. Cell Physiol. **176:** 57–66.

Pereira, R.F., O'Hara, M.D., Laptev A.V., Halford, K.W., Pollard, M.D., Class, R., Simon, D., Livezey, K., and Prockop, D.J. (1998). Marrow stromal cells as a source of progenitor cells for nonhematopoietic tissues in transgenic mice with a phenotype of osteogenesis imperfecta. Proc. Natl. Acad. Sci. USA **95:** 1142–1147.

Pittenger, M.F., Mackay, A.M., Beck S.C., Jaiswal, R.K., Douglas, R., Mosca, J.D., Moorman, M.A., Simonetti, D.W., Craig, S., and Marshak, D.R. (1999). Multilineage potential of adult human mesenchymal stem cells. Science **284:** 143–147.

Prockop, D.J. (1997). Marrow stromal cells as stem cells for nonhematopoietic tissues. Science **276:** 71–74.

Reese, J.S., Koc, O.N., and Gerson, S.L. (1999). Human mesenchymal stem cells provide stromal support for efficient CD34+ transduction. J. Hematother. Stem Cell Res. **8:** 515–523.

Woodbury, D., Schwarz, E.J., Prockop, D.J., and Black, I.B. (2000). Adult rat and human bone marrow stromal cells differentiate into neurons. J. Neurosci. Res. **61:** 364–370.